MEMBRANE TRANSPORT STRUCTURE FUNCTION AND BIOGENESIS:

HCO Salvage Mechanisms in the Submandibular Gland Acinar and Duct Cells

Xiang Luo, Joo Young Choi, Shigeru B. H. Ko, Alexander Pushkin, Ira Kurtz, Wooin Ahn, Min Goo Lee and Shmuel Muallem

J. Biol. Chem. 2001, 276:9808-9816.
doi: 10.1074/jbc.M008548200 originally published online January 3, 2001

THE JOURNAL OF BIOLOGICAL CHEMISTRY
Vol. 276, No. 13, Issue of March 30, pp. 9808–9816, 2001

Printed in U.S.A.

HCO_3^- Salvage Mechanisms in the Submandibular Gland Acinar and Duct Cells*

Received for publication, September 19, 2000, and in revised form, December 4, 2000
Published, JBC Papers in Press, January 3, 2001, DOI 10.1074/jbc.M008548200

Xiang Luo‡§, Joo Young Choi‡§, Shigeru B. H. Ko‡, Alexander Pushkin¶, Ira Kurtz¶, Wooin Ahn‖, Min Goo Lee‖, and Shmuel Muallem‡**

From ‡The Department of Physiology, University of Texas Southwestern Medical Center, Dallas, Texas 75235, ¶The Department of Medicine, Division of Nephrology, ULCA, Los Angeles, California, ‖Department of Pharmacology and Brain Korea 21 Project for Medical Sciences, Yonsei University College of Medicine, Seoul 120-752, Korea

In the present work, we characterized H^+ and HCO_3^- transport mechanisms in the submandibular salivary gland (SMG) ducts of wild type, NHE2−/−, NHE3−/−, and NHE2−/−;NHE3−/− double knock-out mice. The bulk of recovery from an acid load across the luminal membrane (LM) of the duct was mediated by a Na^+-dependent HOE and ethyl-isopropyl-amiloride (EIPA)-inhibitable and 4,4′-diisothiocyanostilbene-2,2′-disulfonic acid (DIDS)-insensitive mechanism. HCO_3^- increased the rate of luminal Na^+-dependent pH_i recovery but did not change inhibition by HOE and EIPA or the insensitivity to DIDS. Despite expression of NHE2 and NHE3 in the LM of the duct, the same activity was observed in ducts from wild type and all mutant mice. Measurements of Na^+-dependent OH^- and/or HCO_3^- cotransport (NBC) activities in SMG acinar and duct cells showed separate DIDS-sensitive/EIPA-insensitive and DIDS-insensitive/EIPA-sensitive NBC activities in both cell types. Functional and immunocytochemical localization of these activities in the perfused duct indicated that pNBC1 probably mediates the DIDS-sensitive/EIPA-insensitive transport in the basolateral membrane, and splice variants of NBC3 probably mediate the DIDS-insensitive/EIPA-sensitive NBC activity in the LM of duct and acinar cells. Notably, the acinar cell NBC3 variants transported HCO_3^- but not OH^-. By contrast, duct cell NBC3 transported both OH^- and HCO_3^-. Accordingly, reverse transcription-polymerase chain reaction analysis revealed that both cell types expressed mRNA for pNBC1. However, the acini expressed mRNA for the NBC3 splice variants NBCn1C and NBCn1D, whereas the ducts expressed mRNA for NCBn1B. Based on these findings we propose that the luminal NBCs in the HCO_3^- secreting SMG acinar and duct cells function as HCO_3^- salvage mechanisms at the resting state. These studies emphasize the complexity but also begin to clarify the mechanism of HCO_3^- homeostasis in secretory epithelia.

HCO_3^- is an anion of paramount biological importance. Among other functions, it determines the pH and controls the solubility of proteins and ions in biological fluids. Yet, the mechanism of HCO_3^- secretion at the tissue and cellular levels is poorly understood. This is exemplified in studies of ion transport by cystic fibrosis transmembrane conductance regulator (CFTR)[1]-expressing cells. When stimulated, most CFTR-expressing cells absorb Cl^- and secrete HCO_3^- (1–6). Although the mechanism of Cl^- absorption by these cells has been extensively studied, few studies have examined the mechanism of HCO_3^- secretion (1–6).

Commonly, fluid and electrolyte secretion by epithelia occurs in two steps. Acinar cells secrete a plasma-like fluid containing about 140 mM NaCl and 25 mM HCO_3^- into the duct lumen. The duct absorbs the Cl^- (and sometime the Na^+, as is the case in the lung (3) and the submandibular salivary gland (SMG) (1)) and secretes as much as 140 mM HCO_3^- (1, 2, 5, 6). CFTR plays a prominent role in Cl^- absorption and HCO_3^- secretion, as is evident from the high Cl^--low HCO_3^- in fluids secreted by glands of CF patients (5, 6). Ductal HCO_3^- secretion and Cl^- absorption are tightly coupled (1–4), which is interpreted in most models to mean that Cl^- absorption and HCO_3^- secretion are mediated by a luminal Cl^-/HCO_3^- exchange mechanism (1–4). Recently we showed that CFTR regulates Cl^-/HCO_3^- exchange activity in model systems (7) and native cells (8).

At the resting state HCO_3^--secreting cells and tissues need to salvage the HCO_3^- leaking to or entering the duct lumen. That is, HCO_3^--secreting cells should have HCO_3^--absorbing mechanisms that are active in the resting state and are inhibited in the stimulated state. There is no knowledge in acinar cells and very little is known of the molecular and functional nature of these mechanisms in duct cells of any secretory gland. Early work with the rat SMG duct identified a ductal Na^+/H^+ exchange activity with pharmacological characteristics of isoform 2 of the NHE family (NHE2) (9, 10). Subsequently, we used RT-PCR analysis and immunocytochemistry to show expression of NHE1 in the basolateral membrane (BLM) and NHE2 and NHE3 in the luminal membrane (LM) of the rat SMG duct (11). A similar approach was used to report expression of NHE1 in the BLM and NHE3 in the LM of the rat parotid gland duct (12). Nevertheless, based on functional assays and pharmacological characterization, we concluded that only NHE1 and NHE2 are functional in the SMG duct (11), and Park *et al.* (12)

* This work was supported in part by National Institutes of Health Grants DE12309 and DK38938 (to S. M.), Basic Research Program of the Korea Science and Engineering Foundation Grant 2000-2-21400-002-1 (to M. G. L.), National Institutes of Health Grant DK46976, and by the Iris and B. Gerald Cantor Foundation, the Max Factor Family Foundation, the Verna Harrah Foundation, the Richard and Hinda Rosenthal Foundation, and the Fredericka Taubitz Foundation (to I. K.) The costs of publication of this article were defrayed in part by the payment of page charges. This article must therefore be hereby marked "*advertisement*" in accordance with 18 U.S.C. Section 1734 solely to indicate this fact.

§ These authors contributed equally to this work.

** To whom correspondence should be addressed: Dept. of Pharmacology, Yonsei University College of Medicine, 134 Sinchon-Dong, Seoul 120-752, Korea. Tel.: 82 2 361 5221; Fax: 82 2 313 1894; E-mail: mlee@yumc.yonsei.ac.kr.

[1] The abbreviations used are: CF, cystic fibrosis; CFTR, cystic fibrosis transmembrane conductance regulator; NHE, Na^+/H^+ exchanger; NBC, Na^+- HCO_3^- co-transporter; WT, wild type; LM, luminal membrane; BLM, basolateral membrane; SMG, submandibular gland; DIDS, 4,4′-diisothiocyanostilbene-2,2′-disulfonic acid; bp, base pairs; BCECF-AM, 2′7′-bis (carboxyethyl)-5-carboxyfluorescence)-acetoxy methyl; RT-PCR, reverse transcriptase-polymerase chain reaction.

conclude that NHE1 and NHE3 are functional in the parotid duct. In a more recent work, we used animals in which the *NHE2* and the *NHE3* genes were disrupted to show that NHE3 and a novel, unidentified Na^+-dependent HOE 694 (HOE)- and EIPA-sensitive mechanism mediate HCO_3^- salvage mechanism in the pancreatic duct (13). However, these studies (13) did not identify the novel luminal Na^+-dependent, HOE- and EIPA-sensitive mechanism and did not exclude the possibility that disruption of one gene resulted in a compensatory up-regulation of the second gene to increase luminal NHE activity back to normal, thus resulting in a lack of phenotype in ducts from NHE2−/− and/or NHE3−/− mice.

H^+/HCO_3^- transport mechanisms by acinar cells are only partially known, and their possible role in transcellular HCO_3^- transport is completely unknown. Salivary gland (11, 12) and pancreatic acinar cells (14) express NHE1 in the basolateral membrane. Na^+/HCO_3^- cotransport (NBC) activity of pancreatic acinar cells (14, 15) was attributed recently to the pancreatic NBC isoform pNBC1 (16). An antibody that recognizes kNBC1 and pNBC1 was used to suggest localization of the protein in the BLM (17, 18). Which NBC isoforms are expressed in salivary gland acinar and duct cells, their properties, and physiological roles are not known.

In the present work, we first analyzed H^+/HCO_3^- transport in interlobular and the microperfused main SMG ducts from WT, NHE2−/−, NHE3−/−, and NHE2−/−;NHE3−/− double knock-out mice. We found functional NHE1-like activity in the BLM, and although expressed in duct cells, neither NHE2 nor NHE3 participates in H^+/HCO_3^- fluxes by these cells. Measurement of Na^+-dependent H^+/HCO_3^- transport showed that in the absence of HCO_3^- SMG acinar cells recovered from an acid load by a mechanism that was inhibited by HOE and EIPA with an IC_{50} of 130 and 23 nM, respectively. HCO_3^- activated two transporters, a DIDS-sensitive and EIPA-insensitive and a DIDS-insensitive mechanism that was inhibited by EIPA with an IC_{50} of about 1.3 μM. Duct cells also expressed similar mechanisms except that the mechanism with the IC_{50} for EIPA of 1.3 μM in the LM transported both OH^- and HCO_3^-. RT-PCR analysis and immunolocalization showed that pNBC1 is expressed in the BLM of SMG acinar and duct cells, consistent with the presence of a DIDS-sensitive/EIPA-insensitive mechanism in these cells. Acinar and duct cells also expressed selective NBC3 splice variants. NBC3 was localized to the LM of both cell types and may account for the cell-specific DIDS-insensitive/EIPA-sensitive Na^+-dependent HCO_3^- or OH^-/HCO_3^- transport by acinar and duct cells, respectively.

EXPERIMENTAL PROCEDURES

Materials and Solutions—2′7′-bis (carboxyethyl)-5-carboxyfluorescein)-AM (BCECF-AM) and H_2DIDS were from Molecular Probes, and collagenase CLS4 was from Worthington, Freehold, NJ. EIPA was from Research Biochemicals International, and DIDS was from Sigma. HOE 694 was a generous gift from Dr. Hans Lang, Avertis, Frankfurt am Main, Germany. Two affinity-purified polyclonal antibodies were raised against synthetic peptides derived from the N terminus of pNBC1: pNBC1a (amino acids 1–19) and pNBC1b (amino acids 51- 69, coupled to an N-terminal cysteine). The affinity-purified polyclonal antibody to kNBC1 was raised against a synthetic peptide corresponding to amino acids 11–24, coupled to an N-terminal cysteine. The polyclonal antibody against NBC3 was raised against a synthetic peptide corresponding to amino acids 1197–1214 of the C terminus of NCB3 (19). This sequence is almost identical to the C-terminal sequence of the known rodent NBC3 splice variants (20). The standard perfusion solution (solution A) contained 140 mM NaCl, 5 mM KCl, 1 mM $MgCl_2$, 1 mM $CaCl_2$, 10 mM HEPES (pH 7.4 with NaOH), and 10 mM glucose. Na^+-free solutions were prepared by replacing Na^+ with *N*-methyl-D-glucamine$^+$. HCO_3^--buffered solutions were prepared by replacing 25 mM NaCl or *N*-methyl-D-glucamine$^+$-Cl^- with 25 mM $NaHCO_3$ or choline-HCO_3, respectively, and reducing HEPES to 5 mM. HCO_3^--buffered solutions were gassed with 5% CO_2, 95% O_2. The osmolarity of all solutions was adjusted to 310 mosmol with the major salt. Animals were anesthetized (40 mg/kg) or killed (200–250 mg/kg) by intraperitoneal injection of sodium pentobarbital and cervical dislocation according to NIH Guidelines for the Care and Use of Laboratory Animals.

Animals and Preparation of Cells—Mice with targeted disruption of the *NHE2* and *NHE3* genes were generated as described previously (21, 22). Heterozygote NHE2+/−;NHE3+/− mice were mated to generate the homozygote double knock-out NHE2−/−;NHE3−/− mice. Animals were typed by tail DNA before use. Deletion of the proteins was verified by Western blot (23) and immunocytochemistry (11, 12). Animals had free access to food and water and were used at 1–2 months of age.

The procedures for preparation of isolated interlobular ducts and acini and for preparation and perfusion of the main SMG duct were similar to those described before (11). In brief, for preparation of a mixture of acini and interlobular ducts, the mouse SMGs were removed into solution A supplemented with 10 mM sodium pyruvate, 0.02% trypsin inhibitor, and 0.1% bovine serum albumin (PSA), minced, and digested in the same solution that contained 0.5 mg/ml collagenase CLS4. The digested tissue was washed three times with PSA, and the cells were used for measurement of pH_i. For perfusion of the main duct, the mice were anesthetized, and the SMGs were exposed and cleared of connective tissue around the ducts. The ducts were cut and transferred to a perfusion chamber and prepared for luminal and bath perfusion. For pH_i measurement, ducts were loaded with BCECF by including the BCECF-AM in the luminal perfusate.

Measurement of pH_i—Isolated ducts and acini were incubated with 2 μM BCECF-AM for 10 min at room temperature, washed once with PSA, and kept on ice until plating on coverslips in the perfusion chamber. Fluorescence of isolated cells or the perfused ducts was measured by photon counting using a Photon Technology International system. BCECF fluorescence was recorded at excitation wavelengths of 440 and 490 nm and an emission wavelength above 530 nm. The 490/440 fluorescence ratios were calibrated using the high potassium nigericin procedure described before (11, 14).

RT-PCR Analysis of NBC3 Splice Variants—For preparation of mRNA, digested cells were placed in a Petri dish, and about 30–50 acinar clusters of 3–5 cells or small duct fragments were collected by glass micropipettes pre-soaked in solution A containing 25 mg/ml bovine serum albumin. This procedure was used to avoid possible contamination of the preparations with nerve terminals and blood vessels and contamination of acinar and duct cells with each other. The cells were ejected into an mRNA extraction solution to prepare mRNA and then cDNA, as detailed before (11). The PCR primers used to detect the transcripts shown in Fig. 5 are as follows: β-actin sense, TGTTACCAACTGGGACGACA, antisense, TCTCAGCTGTGGTGGTGAAG (392 bp); pNBC1 sense, ATGTGTGTGATGAAGAAGAAGTAGAAG, antisense, GACCGAAGGTTGGATTTCTTG (622 bp); kNBC1 sense, CACTGAAAATGTGGAAGGGAAG, antisense, GACCGAAGGTTGGATTTCTTG (531 bp); NBCn1B+D sense, CTGACCCTCACTTGCTTGAA, antisense, CTATGTCTTCCTCAGGCGGAT (342 bp); NBCn1C sense, ATAGGGAAAGGCCTGTCAGCCTC, antisense, GAGAAGCCAAAATCCCTGG (389 bp); NBCn1B sense, TCCGATGCCAGTTCTATATGG, antisense, CAGGGCTATATTTTAGGGTC (473 bp); NBCn1C+D sense, AGAGCAGAAGAATGAGGAA, antisense, TCATGGAAAGTGCCTTCCAC (2.54 kilobase pairs); NBCn1D sense, CTGACCCTCACTTGCTTGAA, antisense, TCATGGAAAGTGCCTTCCAC (2.9 kilobase pairs). Except for NBCn1C+D and NBCn1D, the conditions for all PCR reactions were a hot start of 3 min at 95 °C followed by 35 cycles of 1 min at 94 °C, 90 s at 58 °C, and 1 min at 72 °C. Reactions were terminated by a 5-min incubation at 72 °C and cooling to 10 °C. For NBCn1C+D and NBCn1D, the 35 cycles were 1 min at 94 °C, 150 s at 60 °C, and 150 s at 72 °C. All short amplified PCR products were isolated and sequenced to verify their identity. Between 600–700 bases were sequenced from each end of NBCn1C+D and NBCn1D fragments and found to be 100% identical to the corresponding sequences. The NBCn1C+D primers were used to ascertain the lack of mRNA for these NBC3 splice variants in the duct.

Immunocytochemistry—Isolated cells and tissue sections were placed on a polylysine-coated glass coverslips and allowed to attach for at least 30 min at room temperature before fixation and permeabilization with cold methanol. The staining procedure and various solutions used are listed in Refs. 11 and 13. All primary antibodies used in the present work were affinity-purified. Each of the primary antibodies was incubated with the peptide used to raise the antibodies, and the peptide-blocked antibodies were used as controls. The antibodies were used at a 1:250–1:500 dilution and detected by a fluorescein-tagged secondary donkey anti-rabbit antibodies. Images were collected by a Bio-Rad MRC 1024 confocal microscope.

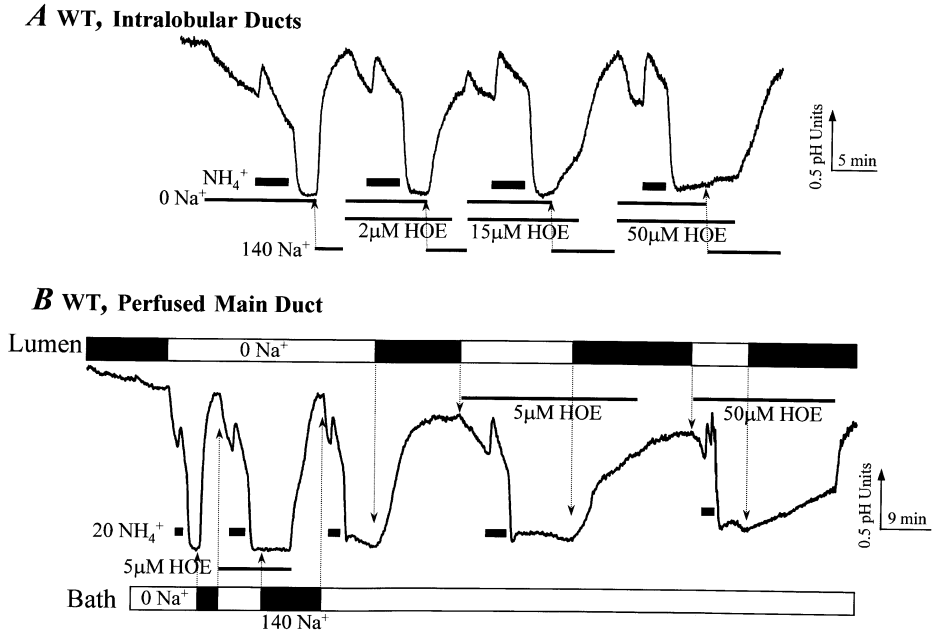

FIG. 1. **Localization of HOE-sensitive transporters in the mouse SMG duct.** Intralobular ducts (*panel A*) loaded with BCECF were perfused with solution A containing 140 mM NaCl. At the time indicted by the *bars*, the ducts were perfused with a Na^+-free solution and transiently exposed to 20 mM NH_4^+ to reduce pH_i to about 6.6. Na^+-dependent pH_i recovery was measured by perfusing the ducts with solution A. The effect of HOE on the rate of recovery from pH_i was measured by including the indicated concentration of HOE in the perfusate. The first derivative of the ascending portion of each trace was used to calculate the effect of HOE, and the results of multiple experiments are plotted in Fig. 4. In *panel B*, the main duct of the mouse SMG was perfused with separate bath and luminal solutions. *Filled columns* indicate perfusion with solution A containing 140 mM NaCl, and *open columns* indicate perfusion with Na^+-free solutions. NH_4^+ was included in the bath solution. As indicated by *bars*, the bath and luminal solutions also contained 5 or 50 μM HOE. Similar results were obtained with at least eight ducts from WT mice.

RESULTS AND DISCUSSION

NHEs in the Mouse SMG Duct—Previous work reported an EIPA- and HOE-sensitive, Na^+-dependent H^+ efflux (or OH^- influx) mechanism in isolated rat SMG acinar and duct cells (11, 24). Fig. 1 extends these findings to cells from the mouse SMG so that mice with disrupted genes can be used to study the role of the transporters of interest in cellular $H^+/OH^-/HCO_3^-$ fluxes. Fig. 1*A* shows measurement of Na^+-dependent pH_i increase in intralobular duct fragment isolated from the SMG of a WT mouse. The ducts were acidified by a transient exposure to a solution containing 20 mM NH_4^+ and incubation in a Na^+-free solution. pH_i increase was initiated by perfusing the ducts with a Na^+-containing solution. The ducts were treated with different concentrations of the NHE inhibitor HOE 694 (HOE) to measure the sensitivity of the Na^+-dependent pH_i increase to HOE. Similar experiments were performed with acinar cells, and all experiments are summarized in Fig. 4 below. In the absence of HCO_3^-, the Na^+-dependent recovery from an acid load in acinar cells is about 20-fold more sensitive to HOE than that in duct cells. Fig. 1*B* shows the HOE sensitivity of the Na^+-dependent H^+ efflux (or OH^- influx) in the BLM and LM of the perfused mouse SMG duct. Similar to findings with the rat SMG (11), the BLM activity was completely inhibited by 5 μM HOE. By contrast, 50 μM HOE were needed to inhibit the LM activity by about 86 ± 11% (n = 7).

Fig. 1 indicates that the mouse SMG duct expresses HOE-sensitive, Na^+-dependent H^+/OH^- transporters in both the BLM and the LM. RT-PCR analysis with mRNA preparations from the mouse SMG acinar and duct cells, similar to that we reported for the rat SMG cells (11) and the mouse pancreatic duct (13), showed that the mouse SMG acinar cells express mRNA for NHE1, and the mouse SMG duct expresses mRNA for NHE1, NHE2, and NHE3 but not for NHE4 and NHE5 (not shown). Based on the sensitivity to HOE of the known NHE isoforms (25), the results in Fig. 1*B* suggest that the duct expresses functional NHE1 in the BLM and NHE2 in the LM. However, further analysis of Na^+-dependent H^+/OH^- transport in ducts from NHE knockout mice showed that this is not the case. Fig. 2 shows individual examples, and Fig. 4 summarizes the results of multiple experiments performed with SMG ducts prepared from NHE2−/− and NHE3−/− mice. The Na^+-dependent H^+/OH^- fluxes and their sensitivity to HOE were the same in SMG ducts of WT, NHE2−/−, and NHE3−/− mice.

The results in Fig. 2 are different from those obtained in the kidney proximal tubule (23) and the pancreatic duct (13), in which deletion of NHE3 reduced the rate of Na^+-dependent H^+/OH^- fluxes across the LM by about 50%. One possibility is that deletion of NHE3 from the SMG resulted in a compensatory increase in NHE2 activity. To address this possibility, we obtained a double NHE2−/−;NHE3−/− knock-out mice and measured H^+/OH^- fluxes in SMG acinar and duct cells of these mice. Figs. 3*A* and 4 show that the HOE sensitivity of Na^+-dependent H^+/OH^- fluxes in SMG intralobular ducts of WT and NHE2−/−;NHE3−/− mice are no different. Fig. 3*B* shows that in the absence of HCO_3^-, 2 μM HOE inhibited better than 90% (n = 3) of NHE activity in SMG acinar cells of NHE2−/−; NHE3−/− mice. Finally, Fig. 3*C* shows that the properties of the BLM and the LM H^+/OH^- fluxes in the main SMG duct of the NHE2−/−;NHE3−/− mice are not different from those found for the SMG ducts of WT mice (Fig. 1).

Semi-quantitative RT-PCR analysis and immunolocalization led us (11) and others (12) to conclude expression of functional NHE1 in the BLM of acinar and duct cells, NHE2 in the LM of SMG and NHE3 in the LM of the parotid gland (11, 12) ducts. As indicated above, RT-PCR analysis with mRNA prepared from SMG intraolublar duct fragments, collected individually with micropipettes to ensure the origin of mRNA, showed expression of NHE1, NHE2, and NHE3 in the mouse SMG duct, confirming the immunolocalization of these proteins in the mouse SMG (11). Measurement of H^+/OH^- fluxes and their inhibition by amiloride analogs such as EIPA (9, 10, 12) or HOE (Ref. 11 and the present work), further suggested expression of functional NHE1 in the BLM and NHE2 and/or NHE3 in the LM of the ducts. Therefore, it was quite surprising to find that deletion of NHE2, NHE3 or both proteins had no measurable effect on the Na^+-dependent, HOE-inhibitable H^+/OH^- fluxes in either the BM or LM of the mouse SMG duct.

Of particular significance is the similar HOE sensitivity of the H^+/OH^- fluxes in the SMG ducts of all animals. This makes it unlikely that the similar rates of H^+/OH^- fluxes are due to compensatory increase in the activity of any NHE transporter. In this case, we would have seen a change in the apparent affinity for HOE. These findings indicate that previous conclusions concerning the identity of the proteins mediat-

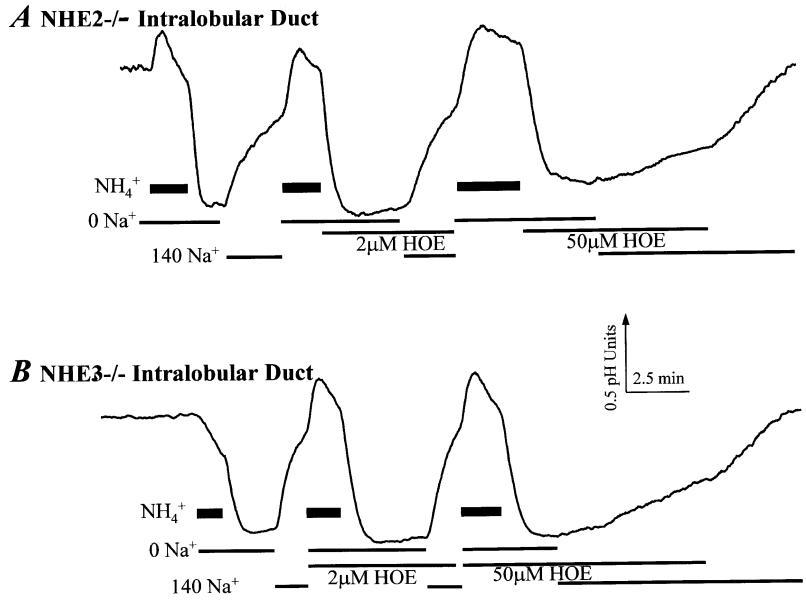

FIG. 2. **Na^+-dependent recovery from an acid load in ducts from the SMG of NHE2−/− and NHE3−/− mice.** The protocol of Fig. 1*A* was used to measure the effect of different concentrations of HOE on Na^+-dependent recovery from an acid load in the SMG intralobular ducts of NHE2−/− (*A*) or NHE3−/− mice (*B*). Similar experiments were performed with at least five ducts obtained from three mice of each genotype and are plotted in Fig. 4.

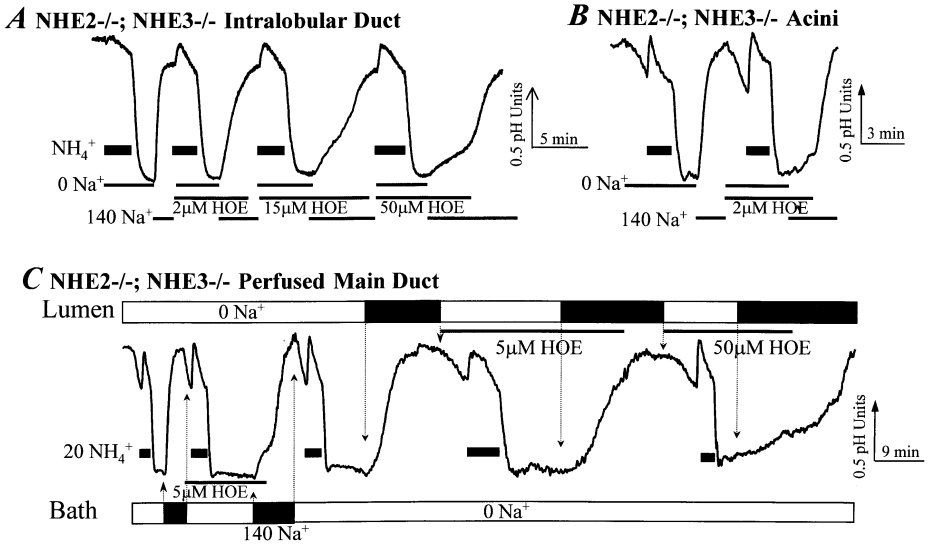

FIG. 3. **Na^+-dependent recovery from an acid load in acini and ducts from the SMG of NHE2−/−;NHE3−/− double knock-out mice.** The protocol of Fig. 1*A* was used to evaluate the HOE sensitivity of the Na^+-dependent recovery from an acid load of intralobular ducts (*A*) or acini (*B*) prepared from the SMG of NHE2−/−;NHE3−/− mice. Similar experiments were performed with ducts obtained from four animals, and acini were obtained from three animals. The protocol of Fig. 1*B* was used to measure the effect of basolateral and luminal HOE on the Na^+-dependent pH_i recovery of acidified main SMG ducts (*C*). Similar results were obtained with four ducts from four animals.

ing H^+/OH^- flux in the LM of salivary gland ducts are not correct (9–12). Rather, neither NHE2 nor NHE3 contribute to H^+/OH^- fluxes across the LM of the SMG duct, and HOE probably inhibits the activity of a H^+/OH^- transporter other than NHE2 and NHE3. This protein is expressed in the SMG duct and has the same activity and HOE sensitivity in ducts from WT and all knock-out animals. The role of NHE2 and NHE3 in salivary gland function remains a mystery.

NBC Isoforms in the Mouse SMG Acinar and Duct Cells—In an effort to identify the novel H^+/OH^- flux activity in the LM of the SMG duct and better understand H^+/OH^- transport by acinar cells, we decided to characterize the Na^+-HCO_3^- cotransporters (NBC) and NBC activity in these cells. A major incentive in doing so was the finding that NBC3 transports H^+/OH^- in a DIDS-insensitive, EIPA-inhibitable manner (19), which is reminiscent of the H^+/OH^- flux activity in the LM of the proximal tubule (23), pancreatic duct (13), and SMG duct (Ref. 11 and present work). Several NBC isoforms have been identified in recent years and are classified based on their activity as the electrogenic kNBC1 (26) and pNBC1 (16) and the electroneutral hNBC3 (19) and the rat NBC3 splice variants NBCn1B, NBCn1C, and NBCn1D (20). Shown in Fig. 5 is an RT-PCR analysis of the known NBC isoforms in SMG acinar

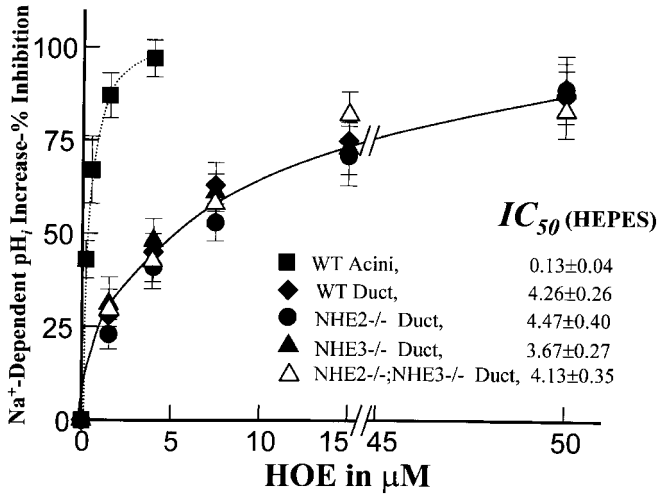

FIG. 4. **HOE sensitivity of Na^+-dependent H^+/OH^- transport by the SMG intralobular duct of WT and mutant mice.** Results of experiments similar to those in Figs. 1–3 were summarized and plotted to calculate the IC_{50} for HOE in acini from WT mice and ducts from WT and mutant mice.

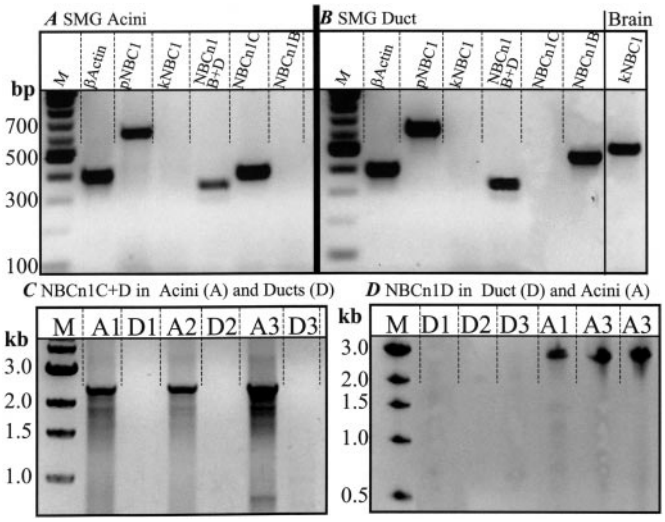

FIG. 5. **RT-PCR analysis of NBC splice variants in SMG acinar and duct cells.** The primers listed under methods were used to amplify the indicated products from mRNA prepared from SMG acini (*A*, *C*, and *D*) or intralobular ducts (*B–D*). An mRNA isolated from brain was used to obtain a positive control for kNBC1 (*B*). Similar results were obtained with at least three separate mRNA preparations from different animals. In *panels C* and *D*, three separate mRNA preparations from SMG acinar (*A1–A3*) or duct (*D1–D3*) cells were used for the RT-PCR reactions. *kb*, kilobases; M, markers.

and duct cells. The mouse SMG acinar and duct cells express mRNA coding for pNBC1 but not for kNBC1. Each of these cell types expresses selective isoforms of the rodent NBCn1. SMG acinar, but not duct, cells express mRNA for NBCn1C and NBCn1D (Fig. 5, *A*, *C*, and *D*). SMG duct, but not acinar, cells express mRNA for NBCn1B (Fig. 5*B*). Primers that detect both NBCn1B+D (fourth *lane* in each blot) detected the expected transcript in mRNA prepared from SMG duct and acinar cells, verifying expression of NBCn1B in the duct. Primers that detect both NBCn1C+D (Fig. 5*C*) detected the expected transcript in mRNA prepared from SMG acinar cells. These primers were used to verify lack of expression of NBCn1C and NBC1D in duct cells.

Next, we used two anti-pNBC1-specific and an anti-NBC3-specific antibodies to localize the proteins by confocal immunofluorescence microscopy. Fig. 6 shows that both cell types express pNBC1 in the BLM. The two anti-pNBC1 antibodies gave similar patterns of staining of the basal and lateral membranes and no staining of the LM, including in the duct. The anti-NBC3 antibodies were raised against a C-terminal peptide (19) that is highly homologous in all NBC3 splice variants (20) and is, thus, likely to detect expression of all NBC3 isoforms. *Panels G–J* of Fig. 6 show that the anti-NBC3 antibodies strongly stained the LM of the SMG ducts. Fig. 6*J* shows that the antibodies also stained the LM and what appears as a web of canaliculi emanating from acinar cells and draining into the intercalated duct. Hence, both the SMG acinar and duct cells express the electroneutral NBC3 in the LM.

In experiments parallel to those in Fig. 6, we used antibodies that specifically recognized kNBC1. These antibodies showed strong staining of the kidney proximal tubule but did not stain any of the cells of the SMG (not shown). Hence, in agreement with the RT-PCR results in Fig. 5, both SMG cell types express only pNBC1 in the BLM.

The lack of luminal Na^+-dependent H^+/OH^- transport phenotype in the ducts of NHE2−/−; NHE3−/− mice may have been due to up-regulation of NBC3 expression. Two findings argue against such an explanation. First, the HOE sensitivity of the luminal mechanisms was the same in ducts from WT and all mutant mice (Fig. 4). Second, we evaluated the level of NBC3 protein expression in cells of mutant mice by immunofluorescence. Fig. 6*L* shows that the level of NBC3 protein is similar in duct and acini of WT and NHE2−/−;NHE3−/− mice.

Na^+-HCO_3^- Cotransport in SMG Acinar and Duct Cells—The kinetic and pharmacological properties of Na^+-HCO_3^- cotransport by the different NBCs are known only to a limited extent. The best characterized are the properties of the electrogenic NBCs. These transporters mediate Na^+-HCO_3^- cotransport with a stoichiometry of 1:3 or 1:2 (27), transport HCO_3^- but not OH^-, are inhibitable by DIDS, and show no sensitivity to amiloride or any amiloride analog (27). When expressed in *Xenopus* oocytes, NBC3 transports OH^- and HCO_3^-, although HCO_3^- transport was faster than OH^- transport (19). HCO_3^- and OH^- transport by NBC3 are not sensitive to DIDS but are inhibited by EIPA (19). NBCn1B expressed in *Xenopus* oocytes mediated an electroneutral Na^+- HCO_3^- cotransport that was not sensitive to either DIDS or EIPA (20). The properties of NBCn1C and NBCn1D are unknown.

Because SMG cells express several NBC isoforms (Figs. 5 and 6), we attempted to develop experimental protocols to isolate the activity of the isoforms based on possible differences in the ability to transport OH^- and HCO_3^- and inhibition by the amiloride analog EIPA. The first set of experiments was performed with SMG acinar cells. Fig. 7*A* shows that in the absence of HCO_3^-, the Na^+-dependent recovery from an acid load by acinar cells was inhibited by EIPA with an IC_{50} of 23 ± 3.7 nM (n = 3), compatible with the activity being mediated by NHE1. Remarkably, HCO_3^- revealed the presence of a base transporter with an IC_{50} for EIPA of about 1.3 μM. Thus, in Fig. 7*A*, 0.5 μM EIPA inhibited recovery from an acid load by about 96 ± 5% in the absence of HCO_3^-, and in the same cells, 1 μM EIPA only partially inhibited recovery from an acid load in the presence of HCO_3^- (n = 5). Experiments similar to that in Fig. 7*B* showed that in the presence of HCO_3^-, EIPA inhibited recovery from an acid load with an IC_{50} of 1.3 ± 0.2 μM (n = 4). To the best of our knowledge, this is the first demonstration of a HCO_3^--dependent shift in EIPA sensitivity of recovery from an acid load. Such a mechanism is reminiscent of the EIPA-sensitive HCO_3^- transporter in vascular smooth muscle cells (28, 29).

An additional finding of note in Fig. 7, *A* and *B*, is that in the absence of HCO_3^-, EIPA completely inhibited recovery from an acid load. By contrast, in the presence of HCO_3^-, EIPA at 30 μM (Fig. 7*B*) or at the highest concentration tested of 100 μM (not shown) did not inhibit more than 67 ± 10% of the recovery from an acid load. This indicates that HCO_3^- was transported by an additional, EIPA-insensitive mechanism. Suspecting that this activity might be mediated by pNBC1, we tested its sensitivity to DIDS. Fig. 8*A* shows that DIDS alone had minimal effect on the recovery from an acid load in the absence of EIPA. However, in the presence of DIDS, EIPA inhibited recovery from an acid load by 93 ± 11% (n = 4), significantly higher than the 67% measured in the absence of DIDS ($p < 0.05$). We reasoned that we were not able to clearly demonstrate an effect of DIDS using the protocol of Fig. 8*A*, since the EIPA-inhibitable transporters mediated the bulk (67%) of the recovery from an acid load. Therefore, we measured the effect of DIDS on the residual EIPA-insensitive HCO_3^- transport. Fig. 8*B* shows that DIDS almost completely inhibited this residual activity.

Using the same protocols with the SMG duct revealed the presence of similar mechanisms with one major and important exception. The base transport mechanism with the higher IC_{50} for EIPA appears to transport both OH^- and HCO_3^-. Hence, Fig. 7, *C* and *D*, shows that the Na^+-dependent recovery from an acid load was inhibited by EIPA with similar a IC_{50} value in

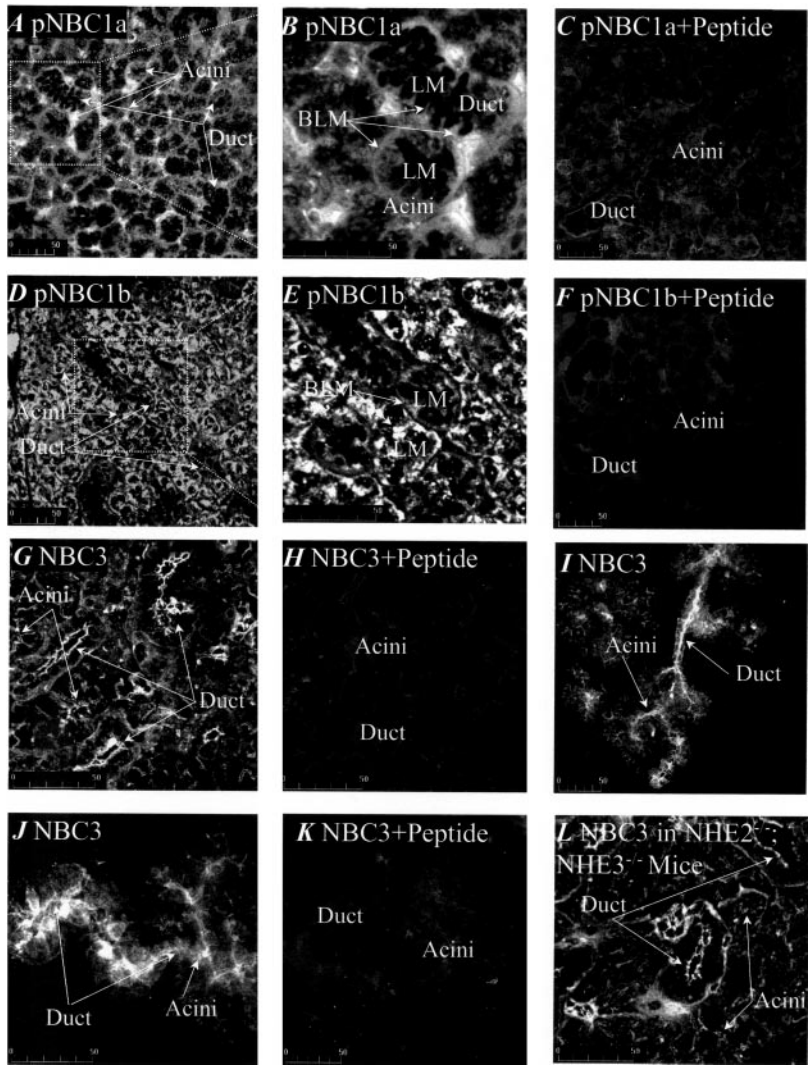

FIG. 6. **Immunolocalization of pNBC1and NBC3 in SMG cells.** Frozen sections (*A–H* and *L*) or isolated cell clusters (*I–K*) were fixed and stained with two different antibodies that recognize pNBC1 (antibodies a (*A–C*) and antibodies b (*D–F*)) and antibodies that recognize all NBC3 isoforms (*G–L*). For controls, the peptides used to raise anti-pNBC1a (*C*), anti-pNBC1b (*F*), and anti-NBC3 (*H* and *K*) were incubated with the respective antibodies before use. Similar staining patterns were observed in at least four experiments with each of the antibodies. Antibodies specific for kNBC1 showed strong staining of the kidney proximal tubule but did not stain any of the cells of the SMG (not shown). Note that in *panels A–K*, cells were from SMG of WT mice, whereas in *panel L*, cells were from SMG of NHE2−/−;NHE3−/− double knock-out mice.

the presence (1.3 ± 0.3 μM, $n = 3$) and absence (1.4 ± 0.3 μM, $n = 5$) of HCO_3^-. This indicates that, unlike the case in acinar cells (Fig. 7, *A* and *B*), HCO_3^- did not reveal the activity of a new transporter. Rather, HCO_3^- appears to be transported by the same Na^+-dependent, EIPA-sensitive mechanism that alkalinized the cells in the absence of HCO_3^-. Fig. 8*C* shows that the residual EIPA-insensitive transport in the presence of HCO_3^- was inhibited by 0.5 mM DIDS.

Functional localization of OH^-/HCO_3^- Transporters—The perfused duct afforded us the ability to functionally localize the OH^-/HCO_3^- transporters in the BLM and LM. Fig. 9 shows the series of experiments performed with the perfused main SMG duct toward achieving this goal. The first part of Fig. 9*A* shows how the effect of HCO_3^- on the rate of BLM $H^+/OH^-/HCO_3^-$ fluxes was estimated. The same ducts incubated in HEPES and then HCO_3^--buffered media were acidified to approximately the same initial pH_i of about 6.6. At this pH_i and at 5% CO_2, the intracellular HCO_3^- concentration is 3.81 mM, which increases the cytosolic buffer capacity from about 38 to 46.7 mM/pH unit. Calculating the ratio of slopes b/a and correcting for the effect of HCO_3^- on buffer capacity indicates that HCO_3^- increased the rate of BLM-located, Na^+-dependent recovery from an acid load by about 1.87 ± 0.25 ($n = 3$)-fold. Exposing the BLM to 10 μM EIPA, which is sufficient to completely inhibit the BLM mechanisms mediating recovery from an acid load in HEPES-buffered medium, inhibited recovery from an acid load in the presence of HCO_3^- by 57 ± 11% (ratio of slopes c/b). Subsequent incubation of the BLM with 10 μM EIPA and 0.25 mM H_2DIDS inhibited the residual, EIPA-independent recovery from an acid load by 71 ± 8% (ratio of slopes d/c). About 10% of the recovery from an acid load was not sensitive to 10 μM EIPA and 0.25 mM H_2DIDS.

The results in Figs. 1 and 9*A* indicate that a transporter with HOE and EIPA sensitivity typical of NHE1 is functional in the BLM of the SMG duct. This is consistent with immunolocalization of NHE1 in the BLM of the mouse SMG ducts (11) and with a recent report of impaired pH_i regulation in parotid acinar cells of NHE1−/− mice (30). Fig. 9*A* indicates that HCO_3^- served as a substrate for a transporter that is not inhibited by EIPA and is inhibited by H_2DIDS, consistent with expression of pNBC1 in the BLM of the SMG duct seen in Fig. 6. Acid-base fluxes mediated by NHE1 and pNBC1 appear to account for about 90% of $H^+/OH^-/HCO_3^-$ transport in the BLM of the SMG duct. As in many other cell types (25), the main function of NHE1 is probably housekeeping, maintaining pH_i around 7.3. pNBC1 is likely to provide the pathway for HCO_3^- influx across the BLM needed for stimulated HCO_3^- secretion across the LM. The best evidence for such a role for pNBC1 is in the pancreatic duct, in which basolateral DIDS inhibited secretin-stimulated HCO_3^- secretion (31, 32).

The effects of HCO_3^- on $H^+/OH^-/HCO_3^-$ fluxes across the LM are shown in Fig. 9, *B* and *C*. Fig. 9*B* shows that 0.25 mM H_2DIDS had no effect on the fluxes. In three experiments, the ratio of the rates of recovery from an acid load in the presence

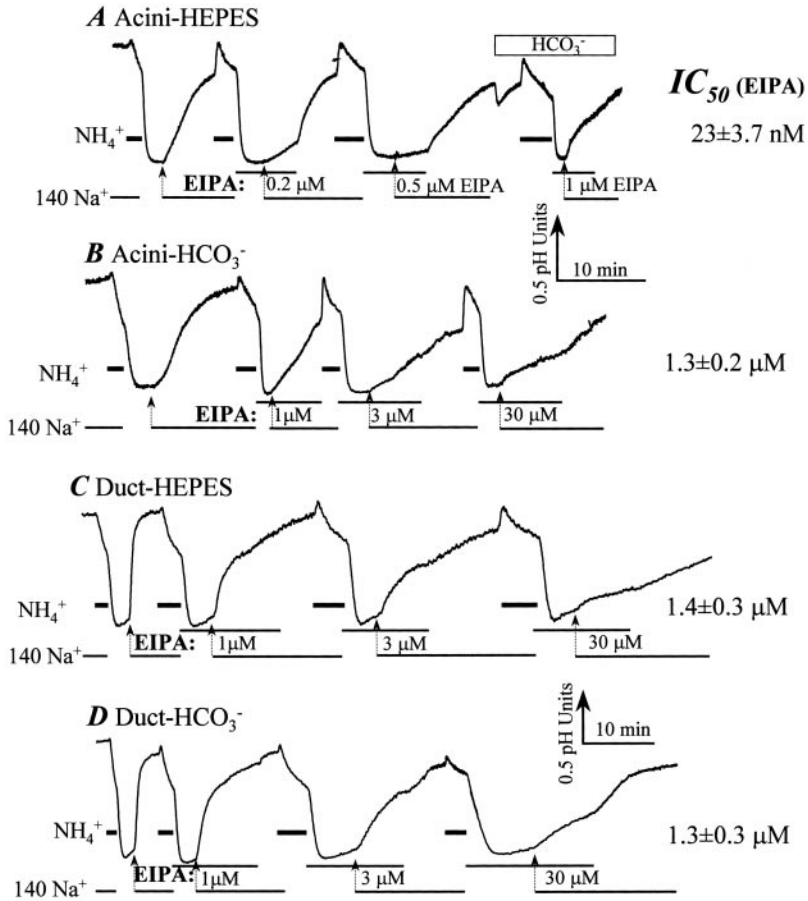

FIG. 7. **EIPA-sensitive HCO_3^- transport in SMG acinar and duct cells.** SMG acini were perfused with HEPES-buffered solutions and in the presence or absence of EIPA at concentrations between 10 nM and 0.5 μM to measure the IC_{50} for EIPA. The acinus in *panel A* was then perfused with a HCO_3^--buffered solution and 1 μM EIPA to demonstrate the effect of HCO_3^- on inhibition of Na^+-dependent pH_i increase by EIPA in the same acinus. In *panel B*, the acini were perfused with HCO_3^--buffered solutions and in the presence or absence of EIPA at concentrations between 0.2 and 100 μM to measure the IC_{50} for EIPA. In *panels C* and *D*, SMG ducts were perfused with HEPES (*C*) or HCO_3^- (*D*)-buffered solutions and in the presence or absence of EIPA at concentrations between 0.2 and 100 μM to measure the IC_{50} for EIPA.

of HCO_3^- and in the presence and absence of H_2DIDS was 0.93 ± 0.14. Fig. 9*C* shows that HCO_3^- increased the rate of recovery from an acid load across the LM by about 1.92 ± 0.21 (n = 5) fold (slope b/a corrected for buffer capacity). However, unlike findings in the BLM, HCO_3^- had no effect on the ability of HOE to inhibit recovery from an acid load. Thus, 50 μM HOE inhibited the rate of recovery from an acid load by 91 ± 8% (n = 4) and 86 ± 9% (n = 7) in the presence and absence of HCO_3^-, respectively. Similarly, 30 μM EIPA inhibited Na^+-dependent recovery from an acid load in the presence of HCO_3^- by about 93 ± 10% (n = 3). This suggests that HCO_3^- did not activate a new HCO_3^- transporter in the LM but, rather, increased the activity of the transporter inhibitable by 50 μM HOE or 30 μM EIPA.

Although none of the findings on its own is sufficient to identify with certainty the transporters in the SMG acinar and duct cells that mediate the Na^+-dependent, DIDS-insensitive HCO_3^- transport that is inhibited by EIPA with an IC_{50} of 1.3 μM, the combined results point to splice variants of the NBC3 family. First, both SMG acinar and duct cells express NBC3 in the LM (Fig. 6), the membrane at which the transport function was localized in the perfused SMG duct. Second, NBC3 can transport both OH^- and HCO_3^- (19), similar to the activity in the duct. Third, OH^- and HCO_3^- transport by NBC3 are inhibited by EIPA but not DIDS (19). Finally, a finding of particular interest is that acini and ducts appear to express different splice variants of NBC3 (Fig. 5). This may explain why in SMG acini a transporter with low affinity for EIPA was observed only in the presence of HCO_3^-. It is possible that the NBC3 splice variants expressed in SMG acinar cells transport HCO_3^- but not OH^-, and the isoform expressed in duct cells transports both HCO_3^- and OH^-.

A significant problem with this interpretation is that NBCn1B was found to transport HCO_3^- but not OH^- and to be insensitive to EIPA (20). However, NBCn1B may behave differently when expressed in the heterologous system of oocytes than in native cells. Furthermore, it is possible that in native cells the NBC3 splice variants do not function individually but rather assemble into complexes to yield the OH^- and/or HCO_3^- transporters with the characteristics found in the present work. In this respect, we note that a Na^+-dependent, DIDS-insensitive/EIPA-sensitive HCO_3^- transporter was found in smooth muscle cells (28, 29) from which the rodent NBC3 splice variants were cloned (20). Further studies with individual and combinations of the NBC3 splice variants are needed to examine this possibility.

In summary, the present work provides new information on the mechanism of $H^+/OH^-/HCO_3^-$ transport and transporters in SMG acinar and duct cells and raises several questions as to the physiological function of the transporters. The present and previous (1, 9–12, 24) molecular, immunological, and functional studies all support the presence of a functional NHE1 in the BLM of salivary gland acinar and duct cells. Molecular and immunological studies provided evidence for the expression of NHE2 and NHE3 in the LM of duct cells (11, 12). Particularly convincing was the finding that disruption of the *NHE2* and *NHE3* genes resulted in deletion of the respective proteins from the mice (11, 12, 23). Inhibition by amiloride and analogs of a Na^+-dependent recovery from an acid load in the absence of HCO_3^- was interpreted as expression of functional NHE2 (10, 11) and/or NHE3 (12) in the LM of the duct. However, the present work clearly shows that this is an erroneous conclusion. Deletion of NHE2 and NHE3 or both proteins had no effect on acid-base fluxes across the luminal membrane or their sensitivity to HOE and EIPA. Therefore, we conclude that NHE2 and NHE3 do not function as H^+ transporters in the LM

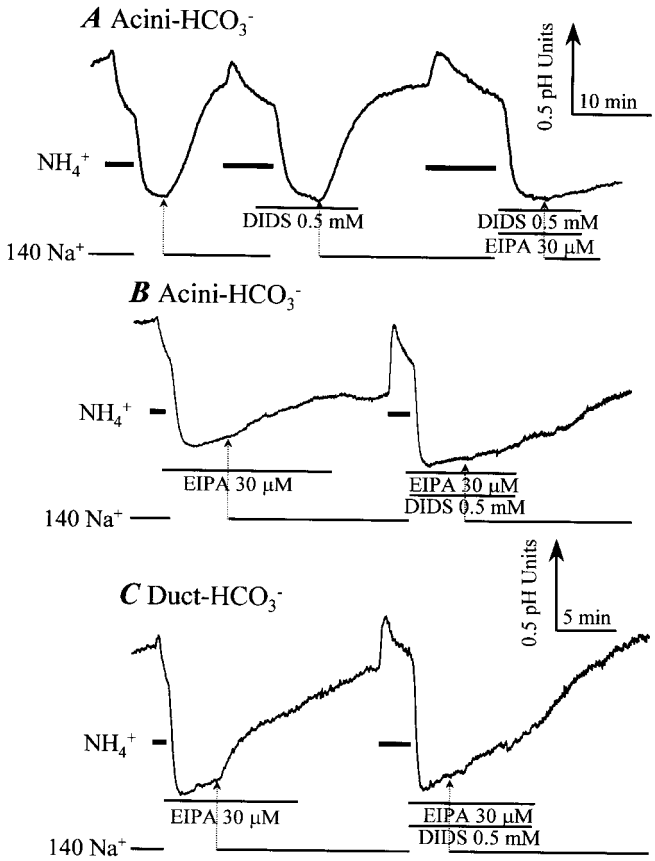

FIG. 8. **EIPA-insensitive, DIDS-sensitive HCO_3^- transport in SMG acinar and duct cells.** Acini (*A* and *B*) and duct fragments (*C*) were perfused in HCO_3^--buffered solutions and, as indicated by the *bars*, solutions containing 0.5 mM DIDS and then DIDS and 30 μM EIPA (*A*) or EIPA and then EIPA and DIDS (*B* and *C*). Similar results were observed in at least three experiments under each condition.

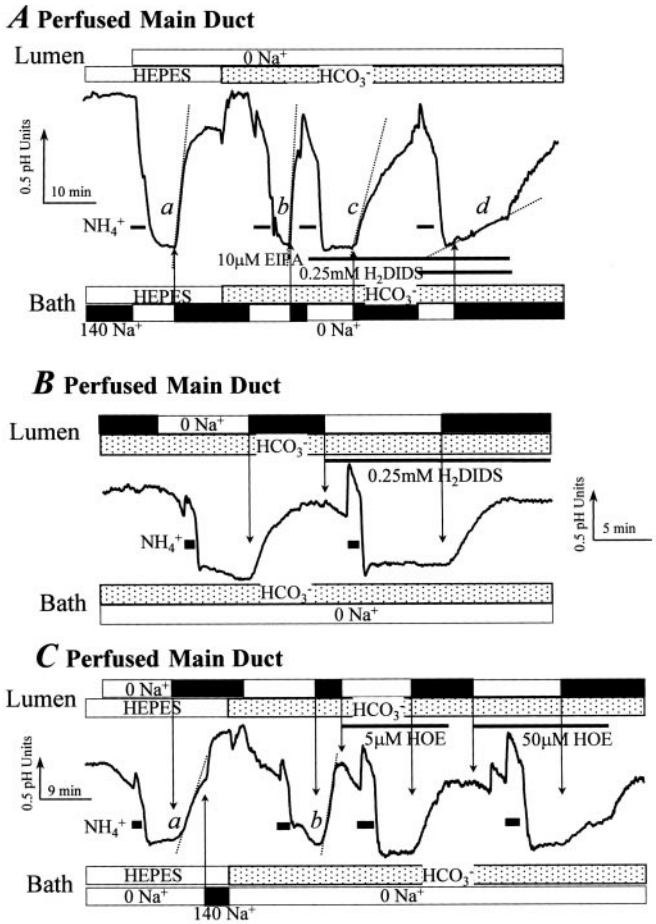

FIG. 9. **Localization of HCO_3^- transporters in the perfused SMG duct. Main SMG ducts were perfused with separate luminal and bath solutions (*A–C*).** In *panel A*, the lumen was perfused with Na^+-free, then HEPES- and HCO_3^--buffered solutions to isolate the Na^+-dependent transporters in the BLM. The bath was perfused first with Na^+-free (*open columns*) or Na^+-containing (*close columns*) HEPES- and then HCO_3^--buffered solutions to evaluate the effect of HCO_3^- on recovery from an acid load (slopes *a*, *b*). At the indicated times, the ducts were perfused with bath solutions containing 10 μM EIPA or EIPA and 0.25 mM H_2DIDS to evaluate the effect of each inhibitor on HCO_3^- transport (slopes *c*, *d*). In *panel B*, the bath was perfused with a Na^+-free HCO_3^--buffered solution to measure the effect of H_2DIDS on luminal, Na^+-dependent HCO_3^- influx. In *panel C*, the bath was perfused with Na^+-free, HEPES-, and then HCO_3^--buffered solutions, and the lumen was perfused with Na^+-free and Na^+-containing, HEPES- and then HCO_3^--buffered solutions to evaluate the effect of HCO_3^- on the rate of recovery from an acid load (slopes *a, b*). At the indicted times, the HCO_3^--buffered luminal solutions contained 5 or 50 μM HOE to demonstrate inhibition of HCO_3^- transport across the LM by HOE.

of the SMG duct. A function for NHE2 could not be found in the proximal tubule (23) or the pancreatic duct (13). Hence, the physiological role of NHE2 and NHE3 in the SMG remains to be found. One possibility is that they lost their function as Na^+-H^+ exchanges in the SMG duct but retained a scaffolding role needed to coordinate H^+/HCO_3^- transport by the SMG duct.

We identified a Na^+-dependent, EIPA-sensitive/DIDS-insensitive H^+/HCO_3^- transport that is not mediated by any known NHE isoform in the kidney proximal tubule (23), the pancreatic duct (13), and now the SMG duct and acinar cells (present work). The present findings suggest that splice variants of NBC3 may mediate the transport in all tissues. An electroneutral Na^+-HCO_3^- cotransport mechanism can function in parallel with the NHE3 in HCO_3^- absorption by the proximal tubule. Indeed, disruption of the NHE3 gene only slightly reduced serum HCO_3^- and had no effect on serum Na^+ (22). Furthermore, 40% of HCO_3^- absorption was retained in proximal tubules of NHE3−/− mice (22, 23). This can be mediated by a splice variant of NBC3 since a Na^+-dependent, EIPA-inhibitable acid-base transporter was found in the proximal tubule of NHE2−/−;NHE3−/− double knockout mice (23).

On the other hand, it appears paradoxical to find Na^+-dependent HCO_3^- absorbing mechanisms in HCO_3^- secreting tissues such as the pancreas (13, 33) and the SMG (Refs. 9–12 and the present work). However, these transporters may function as HCO_3^- salvage mechanisms in the resting state to maintain acidic luminal fluid during periods of low fluid secretion and flow. These tissues secrete digestive enzymes that have pH optima at or above 7.0. During periods of low flow, the digestive enzymes can be activated while in the duct to damage the duct and eventually the tissue, as occurs in chronic pancreatitis (34) and CF (5, 6). In this respect, it is interesting that the Na^+-dependent, EIPA-sensitive mechanism in acinar cells transports only HCO_3^-, whereas that of duct cells transports both OH^- and HCO_3^-. Hence, acinar cells can absorb part of the HCO_3^- present in the fluid secreted under resting conditions. The duct will continue to salvage HCO_3^- by absorbing base equivalent even at low HCO_3^- concentration due to the acidic pH, and thus further reduces the pH of the secreted fluid.

At present, it is unknown how HCO_3^- salvage and secreting mechanisms are regulated in the SMG acinar and duct cells. If the NBC3 splice variants function as HCO_3^- salvage mechanisms in the LM at the resting state and pNBC1 provides the HCO_3^- entry pathway in the BLM during stimulated secretion, we expect secretagogues to stimulate pNBC1 and inhibit NBC3 activities. In the pancreas, Ca^{2+}-mobilizing agonists activated

Cl^-/HCO_3^- exchange and inhibited overall Na^+-HCO_3^- cotransport in pancreatic acini (14, 15), and elevation of cAMP inhibited HCO_3^- salvage mechanisms in the LM of the duct (13). Similar regulatory mechanisms may function in the SMG and other secreting glands. It will be important in the future to examine in greater details the regulation of HCO_3^- salvage and secretion by various cells of secretory glands.

Acknowledgments—We are grateful to Drs. Gary Shull and Patrick Schultheis (University of Cincinnati) for providing us with mating pairs of NHE2+/− and NHE3+/− mice. Karen Miller provided excellent administrative support.

REFERENCES

1. Cook, D. I., van Lennep, E. W., Roberts, M. L., and Young, J. A. (1994) in *Physiology of the Gastrointestinal Tract* (Johnson, L. R., ed) 3rd Ed., pp. 1061–1117, Raven Press, Ltd., New York
2. Argent, B. E., and Case, R. M. (1994) in *Physiology of the Gastrointestinal Tract* (Johnson, L. R., ed) 3rd Ed., pp. 1478–1498, Raven Press, Ltd., New York
3. Pilewski, J. M., and Frizzell, R. A. (1999) *Physiol. Rev.* **79,** S215–S255
4. Grubb, B. R., and Boucher, R. C., (1999) *Physiol. Rev.* **79,** S193–S213
5. Johansen, P. G., Anderson, C. M., and Hadorn, B., (1968) *Lancet* **1,** 455–460
6. Kopelman, H., Corey, M., Gaskin, K., Durie, P., Weizman, Z., and Forstner, G. (1988) *Gastroenterology* **95,** 349–355
7. Lee, M. G., Wigley, W. C., Zeng, W., Noel, L. E., Marino, C. R., Thomas, P. J., and Muallem, S. (1999) *J. Biol. Chem.* **274,** 3414–3421
8. Lee, M. G., Choi, J. Y., Luo, X., Strickland, E., Thomas, P. J., and Muallem, S. (1988) *J. Biol. Chem.* **274,** 14670–14677
9. Paulais, M., Cragoe, E. J., Jr., and Turner, R. J. (1994) *Am. J. Physiol.* **266,** C1594–C1602
10. Chaturapanich, G., Ishibashi, H., Dinudom, A., Young, J. A., and Cook, D. I. (1997) *J. Physiol.* **503,** 583–598
11. Lee, M. G., Schultheis, P. J., Yan, M., Shull, G. E., Bookstein, C., Chang, E., Tse, M., Donowitz, M., Park, K., and Muallem, S. (1998) *J. Physiol.* **513,** 341–357
12. Park, K., Olschowka, J. A., Richardson, L. A., Bookstein, C., Chang, E. B., and Melvin, J. E. (1999)*Am. J. Physiol.* **276,** G470–G478
13. Lee, M. G., Ahn, W., Choi, J. Y., Luo, X., Seo, J. T., Schultheis, P. J., Shull, G. E., Kim, K. H., and Muallem, S., (2000) *J. Clin. Invest.* **105,** 1651–1658
14. Muallem, S., and Loessberg, P. A. (1990) *J. Biol. Chem.* **265,** 12806–12812
15. Muallem, S., and Loessberg, P. A. (1990) *J. Biol. Chem.* **265,** 12813–12819
16. Abuladze, N., Lee, I., Newman, D., Hwang, J., Boorer, K., Pushkin, A., and Kurtz, I. (1998) *J. Biol. Chem.* **273,** 17689–17695
17. Marino, C. R., Jeanes, V., Boron, W. F., and Schmitt, B. M. (1999) *Am. J. Physiol.* **277,** G487–G494
18. Thevenod, F., Roussa, E., Schmitt, B. M., and Romero, M. F. (1999) *Biochem. Biophys. Res. Commun.* **264,** 291–298
19. Pushkin, A., Abuladze, N., Lee, I., Newman, D., Hwang, J., and Kurtz, I. (1999) *J. Biol. Chem.* **274,** 16569–16575
20. Choi, I., Aalkjaer, C., Boulpaep, E. L., and Boron, W. F. (2000) *Nature* **405,** 571–575
21. Schultheis, P. J., Clarke, L. L., Meneton, P., Harline, M., Boivin, G. P., Stemmermann, G., Duffy, J. J., Doetschman, T., Miller, M. L., and Shull, G. E. (1998) *J. Clin. Invest.* **101,** 1243–1253
22. Schultheis, P. J., Clarke, L. L., Meneton, P., Miller, M. L., Soleimani, M., Gawenis, L. R., Riddle, T. M., Duffy, J. J., Doetschman, T., Wang, T., Giebisch, G., Aronson, P. S., Lorenz, J. N., and Shull, G. E. (1998) *Nat. Genet.* **19,** 282–285
23. Shah, M., Lee, M. G., Schulcheis, P. J., Shull, G. E. Muallem, S., and Baum, M. (2000) *J. Clin. Invest.* **105,** 1141–1146
24. Zhao, H., Xu, X., Diaz, J., and Muallem, S. (1995) *J. Biol. Chem.* **270,** 19599–19605
25. Noel, J., and Pouyssegur, J. (1995) *Am. J. Physiol.* **268,** C283–C296
26. Romero, M. F., Hediger, M. A., Boulpaep, E. L., and Boron, W. F. (1997) *Nature* **387,** 409–413
27. Romero, M. F., and Boron, W. F. (1999) *Annu. Rev. Physiol.* **61,** 699–723
28. Bobik, A., Neylon, C. B., Little, P. J., Cragoe, E. J., Jr., and Weissberg, P. L. (1990) *Clin. Exp. Pharmacol. Physiol.* **17,** 297–301
29. Little, P. J., Neylon, C. B., Farrelly, C. A., Weissberg, P. L., Cragoe, E. J., Jr., and Bobik, A. (1995) *Cardiovasc. Res.* **29,** 239–246
30. Evans, R. L., Bell, S. M., Schultheis, P. J., Shull, G. E., and Melvin, J. E. (1999) *J. Biol. Chem.* **274,** 29025–29030
31. Ishiguro, H., Steward, M. C., Lindsay, A. R. G., and Case, R. M. (1996) *J. Physiol.* (*Lond.*) **495,** 169–178
32. Ishiguro, H., Naruse, S., Steward, M. C., Kitagawa, M., Ko, S. H. B., Hayakawa, T., and Case, R. M. (1998) *J. Physiol.* (*Lond.*) **511,** 407–422
33. Zhao, H., Star, R. A., and Muallem, S. (1994) *J. Gen. Physiol.* **104,** 57–85
34. Lerch, M. M., and Gorelick, F. S. (2000) *Med. Clin. N. Am.* **84,** 549–563